Nanoscale

RSC Publishing

PAPER

View Article Online
View Journal | View Issue

Cationic poly(lactic-*co*-glycolic acid) iron oxide microspheres for nucleic acid detection†

Cite this: *Nanoscale*, 2013, **5**, 3800

Chandra Mouli Pandey,[ab] Aditya Sharma,[a] Gajjala Sumana,*[a] Ida Tiwari[b] and Bansi Dhar Malhotra*[ac]

Received 31st December 2012
Accepted 8th February 2013

DOI: 10.1039/c3nr34355c

www.rsc.org/nanoscale

Herein, we envisage the possibility of preparing stable cationic poly(lactic-*co*-glycolic acid) (PLGA) microspheres encapsulating the iron oxide nanoparticles (IONPs; 8–12 nm). The IONPs are incorporated into PLGA in organic phase followed by microsphere formation and chitosan coating in aqueous medium *via* nano-emulsion technique. The average size of the microspheres, as determined by dynamic light scattering are about 310 nm, while the zeta potential for the composite remains near 35 mV at pH 4.0. These microspheres are electrophoretically deposited onto indium tin oxide (ITO)-coated glass substrate used as cathode and parallel platinum plate as the counter electrode. This platform is utilized to fabricate a DNA biosensor, by immobilizing a probe sequence specific to *Escherichia coli*. The bioelectrode shows a surface-controlled electrode reaction with the electron transfer coefficient (α) of 0.64 and charge transfer rate constant (k_s) of 61.73 s^{-1}. Under the optimal conditions, this biosensor shows a detection limit of 8.7×10^{-14} M and is found to retain about 81% of the initial activity after 9 cycles of use.

Introduction

The biomedical applications of nanoscale materials are governed by the fact that they exhibit size compatibility with bio-receptors such as cells, viruses, proteins and nucleic acids.[1] In this context, iron oxide nanoparticles (IONPs) have established a special relevance due to their unique size-dependent magnetic properties, thermal stability, chemical inertness and biocompatible characteristics.[2,3] The use of magnetic particles for biomedical applications offers a number of additional advantages such as control and transport of the bio-assembly to a specific location onto the transducer surface.[4] Furthermore, they can be retained and removed with a magnet without affecting the transducer surface, thus creating possibilities for regeneration and their reuse.[5] Biomedical applications rely on the stability of these particles in physiological conditions, which are, however, limited by their tendency towards aggregation, arising from the strong dipolar interactions among them. It has been reported that the large surface area-to-volume ratio of uncoated IONPs renders them to form clusters *via* agglomeration.[6] In an attempt to overcome the instability of these particles in suspension, much effort has been devoted to their functionalization, effectively in the form of the core–shell system.[7] Potential stabilizing agents including polymers, long-chain carboxylic acids and phosphates are preferred in this regard as they yield thermodynamically stable dispersions of IONPs.[8] Further, the combination of the nanoparticles with polymers that are supplied with active functional groups have attracted much interest as the polymer shell can facilitate the interaction with the biomolecules. In this context, the use of poly(D,L-lactic-*co*-glycolic acid) (PLGA) has been extensively explored to obtain IONPs-embedded PLGA microspheres owing to the strong coordination interaction of the carboxylate group with that of Fe(III).[9–11]

The surface charge of nanoparticles imparts an important effect on their interaction with the biological molecules. Positively charged nanoparticles are reported to allow a higher extent of immobilization, apparently as a result of the ionic interactions established between the particles and anion-rich biomolecules.[12] PLGA-coated nanoparticles exhibit negative charge that can be shifted to neutral or positive charges by surface modification.[11,13] Herein, we explore the possibility of preparing a stable aqueous suspension of PLGA–IONPs microspheres with chitosan (Ch) coating by a nano-emulsion technique. The process involves the formation of a conventional oil-in-water emulsion which consists of an oil phase containing a partially water-miscible solvent, PLGA and IONPs, and an aqueous phase containing Ch. The presence of amino groups in Ch helps in stabilizing the microspheres, which are otherwise unstable as reported in literature.[14–16]

[a]*Biomedical Instrumentation Section, National Physical Laboratory (Council of Scientific & Industrial Research), New Delhi-110012, India. E-mail: sumanagajjala@gmail.com; Fax: +91-11-45609312; Tel: +91-11-45609152*

[b]*Department of Chemistry, Faculty of Sciences, Banaras Hindu University, Varanasi-221005, India*

[c]*Department of Biotechnology, Delhi Technological University, Delhi 110042, India. E-mail: bansi.malhotra@gmail.com; Fax: +91-11-27871023; Tel: +91-11-27871043*

† Electronic supplementary information (ESI) available. See DOI: 10.1039/c3nr34355c

For biosensing application, a precise control over the spatial arrangement and distribution of the nanoparticles onto the substrate is utmost important.[17] Among the various techniques, electrophoretic deposition (EPD) offers rapid deposition of desired materials and their composites with a simple design setup, thereby presenting a scope as an automated and continuous process on an industrial scale.[18] It provides tunable control over the degree of deposition of the charged colloidal particles onto an electrode surface under the influence of an applied electric field. Recent studies highlight the importance of pH change at the electrode surface and demonstrate the possibility of EPD using pH-dependent additives.[19] Chitosan is one of the most studied polymers owing to its pH-responsive behaviour and excellent adhesive property. Under acidic conditions, protonation of the amine groups of this polymer provide effective charge to the colloids necessary to impart a high degree of solubility in polar solvents, such as water and ethanol, through electrostatic stabilization. However, on application of the requisite potential, the repulsion is reduced at the electrode surface, wherein particles coagulate to form a film.[18,19] Zeta potential analysis reveals that the prepared microspheres are positively charged at pH 4.0, which enables their cathodic electro-deposition onto an ITO-coated glass electrode. Subsequently, this microspheres-based platform has been utilized for the fabrication of nucleic acid biosensor by covalent immobilization of the *Escherichia coli* specific amine-terminated DNA as the capture probe. Electrochemical impedance spectroscopy (EIS) has been used for the transduction of the hybridization reaction with complementary target sequence specific to *E. coli* (O157:H7), single-base mismatch, and non-complementary sequences, to investigate the response characteristics of this nucleic acid sensor. To the best of our knowledge, the present work is the first report employing utilization of cationic PLGA microspheres encapsulating IONPs for biosensing application.

Experimental section

Chemicals

Iron(III) acetylacetonate, 1,2-hexadecanediol, oleic acid, oleylamine, glutaraldehyde, PLGA (M_w = 40 000–75 000), 1-ethyl-(dimethylaminopropyl)carbodiimide (EDC), *N*-hydroxysuccinimide (NHS), polyvinyl alcohol (PVA), and chitosan (M_w = 15 000–20 000) were of analytical grade and purchased from Sigma-Aldrich. The details of oligonucleotide DNA sequences and processing of cultures of water-borne pathogens were reported elsewhere.[20]

Synthesis of oleic acid-capped IONPs

IONPs were synthesised by the reported procedure with slight modifications.[21] Briefly, Iron(III) acetylacetonate (4 mmol), 1,2-hexadecanediol (10 mmol), oleic acid (12 mmol), oleylamine (6 mmol), and phenyl ether (20 mL) were mixed at constant stirring at 200 °C for 2 h mechanically under inert nitrogen atmosphere. The obtained black coloured mixture was cooled to room temperature (25 °C) and purified using repeated washing with pure ethanol followed by separation *via* centrifugation. The formed product was dispersed in hexane and the partially dispersed mixture was centrifuged at 10 000 rpm for about 10 min to remove any un-dispersed residue.

Preparation of PlgNPs

PlgNPs were prepared using a nano-emulsion method. For this, a mixture of PLGA (200 mg) and IONPs (30 mg) was dissolved in 10 mL of dichloromethane under continuous stirring.[16] This organic solution was then added to 20 mL of aqueous solution containing PVA (1.0%) and Ch (0.3%) as the stabilizer mixture followed by the addition of EDC (0.4 M) and NHS (0.05 M). Thereafter, the organic–aqueous solution mixture was emulsified for 15 min using an ultrasonicator (Vibronics Pvt. Ltd, Mumbai, India) operated at 24 kHz. Further, the organic solvent was evaporated using a water bath maintained at 40 °C and the solution was subjected to centrifugation (20 000 rpm) for three repetitive cycles.[22,23] Thus prepared PlgNPs were re-suspended in 20 mL of water and stored at 4 °C.

Electrophoretic deposition of PlgNPs onto ITO electrode

The synthesized PlgNPs were cathodically deposited using electrophoretic deposition technique (Bio Rad, Model 200/2.0) onto a pre-hydrolyzed ITO electrode using a two-electrode system, with parallel-placed platinum as the counter electrode. Prior to deposition, the prepared colloidal suspension was diluted with ethanol in a 1 : 2 ratio, of which 12 mL of the aliquot was taken out and subjected to EPD at a DC potential of 5 V for 60 s.[19] The obtained uniform film was repeatedly washed with deionized water and stored in a desiccator. For control experiments, Ch–IONPs electrodes were prepared by EPD of Ch-coated IONPs onto ITO electrodes (Ch–IONPs/ITO) under similar conditions.

Fabrication of nucleic acid-functionalized PlgNPs/ITO electrode

The bioconjugation of aminated probe DNA (pDNA) to the PlgNPs/ITO electrode surface was performed using glutaraldehyde as a cross linker. For this purpose, the PlgNPs/ITO surface was activated by incubation in aqueous glutaraldehyde solution (0.1% v/v) for 1 h followed by washing with deionized water. To allow coupling between the amine terminal of pDNA and the glutaraldehyde-modified PlgNPs/ITO electrode, 20 μL of pDNA was spread onto the modified electrode surface followed by 5 h incubation in a humid chamber at room temperature (25 °C). The pDNA/PlgNPs/ITO bioelectrode was rinsed with Tris–HCl (10 mM) and EDTA (1 mM) buffer solution (TE, pH 8.0) to remove any physically adsorbed pDNA on the electrode surface. The prepared pDNA/PlgNPs/ITO bioelectrodes were utilized for detection of *E. coli* by subjecting them to various concentrations of complementary target DNA for 30 min and the corresponding difference in R_{CT} value was measured by EIS.[24]

Characterization

The X-ray diffraction (XRD) spectrum of the powdered IONPs sample was recorded on a Rigaku instrument over the 2θ range from 25° to 70° using monochromatized X-ray beam with Cu-Kα

radiation ($\lambda = 1.5406$ Å). Field emission transmission electron microscope (TEM, JEOL JEM-2100F), at an accelerating voltage of 200 kV, was used to determine the IONPs size and the formation of PlgNPs. Dynamic light scattering (DLS) measurements were performed with a Zetasizer Nano-ZS90 (Malvern Instruments) at a scattering angle of 90° and constant temperature of 25 °C to determine the particle size and zeta potential of PlgNPs. Contact angle (CA) measurements were done using Data Physics OCA15EC. Fourier transform infrared (FTIR) spectra were recorded using a Perkin-Elmer spectrometer (Spectrum BX) at 25 °C over the frequency range of 4000–400 cm^{-1}. The morphology of the deposited microspheres was determined with scanning electron microscopy (LEO 440) with an accelerating voltage of 10 kV. Electrochemical characterization was carried out by an Autolab Potentiostat/Galvanostat (Eco Chemie, Netherlands) using a three-electrode system with ITO as the working electrode, Ag/AgCl as reference electrode, and platinum foil as counter electrode, in phosphate-buffer (PBS; 50 mM, pH 7.4) containing 5 mM $[Fe(CN)_6]^{3-/4-}$.

Results and discussion

Scheme 1 shows the various steps used for the preparation of PlgNPs, their deposition onto the ITO electrode, and the immobilization of pDNA onto the electro-deposited microspheres. It is known that the uncapped IONPs, due to their high surface energy, clump together and form aggregates in a short duration of time, which cannot be dispersed even by ultrasonication.[23] Keeping this in view, the IONPs were initially capped with oleic acid to render them stable in solution. Further, in the process of preparing PlgNPs, the IONPs were transferred to an organic phase containing PLGA, which coated the particles and made them readily dispersed in organic medium. Oil-in-water emulsion was prepared by adding aqueous Ch solution containing PVA to this PLGA–IONPs solution and the formation of nanosized droplets were induced by sonication.[22,25] The PVA surfactant probably stabilizes these nano-droplets and helps in the uniform chitosan coating to provide stable microspheres.[11] The effect of chitosan concentration was studied till a stable suspension of cationic PlgNPs was obtained, as revealed by zeta potential analysis (Table S1†). Chitosan, present on the surface of the microspheres, has primary amino groups with pK_a values around 6.3, below which most of the amino groups get protonated making PlgNPs dispersed in aqueous medium. At an applied voltage of 5 V between two electrodes for a certain time, Ch experiences a higher pH than pK_a near the cathode, wherein its amino groups are deprotonated and become insoluble resulting in deposition of the PlgNPs onto the ITO substrate.[18]

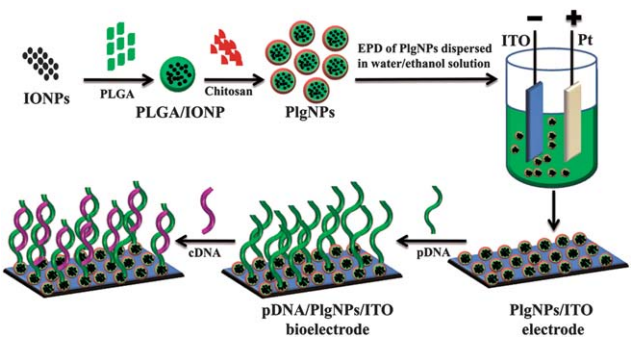

Scheme 1 Schematic illustration for the preparation of PlgNPs, EPD of PlgNPs onto ITO electrode and its application for electrochemical detection of *E. coli*.

The TEM image (Fig. 1; panel i) shows that the oleic acid-capped IONPs are mono-dispersed and nearly spherical in shape having a particle size of 8–12 nm. The results of XRD studies (Fig. 1; panel ii), show the prominent diffraction peaks at (2 2 0), (3 1 1), (4 0 0), (5 1 1), and (4 4 0) with a spinal structure corresponding to Fe_3O_4 or γ-Fe_2O_3 having a face centred cubic crystal lattice (JCPDS no: 87-0245).[26] Except for the broadening of the peaks, all the position and relative intensity of diffraction peaks are identical with the standard spectrum for bulk magnetite. Fig. 1 (panel iii) shows the TEM image of the synthesized PLGA–IONPs in which the IONPs are slightly aggregated within the PLGA microspheres, which may perhaps be due to evaporation of the particles on the TEM grid. It can be seen that when these PLGA–IONPs are treated with Ch in aqueous phase, there is formation of a polymer layer of about 10 nm around the surface of the PLGA–IONPs (Fig. 1; panel iv). The average size of formed PlgNPs is about 310 nm with a polydispersity index of ~0.4 as can be seen from the results of DLS measurements (Fig. 2; panel i). It has been reported that factors like the size of the vials that are used for making the emulsions, sonication intensity, the position of the sonicator head in the solution, and the duration of sonication, influence the size of the microspheres. In general, longer sonication times and higher sonication powers may result in the formation of smaller spheres.[22] To determine the particle stability, zeta potential measurements have been conducted as a function of pH at 25 °C, indicating the isoelectric point of the PlgNPs to be 7.3 (Fig. 2; panel ii). At pH values sufficiently different from the isoelectric point, the particles are stabilized by electrostatic repulsions. Further, the zeta potential measurements reveal that the complex is positively charged with a zeta potential of about 35 mV at the pH value of 4.0, indicating the stability of this composite at this pH (Fig. 2; inset panel ii).

FTIR spectroscopic analysis has been carried out to characterize the capping of organic oleate in the synthesized IONPs and the formation of PLGA–IONP composites. As shown in Fig. 3 (curve i), the wide band in the range of 3130–3630 cm^{-1} is assigned to O–H vibrations. The characteristic absorption peak of Fe–O is observed at 583 cm^{-1}. The sharp bands seen at 2924 and 2854 cm^{-1} are attributed to asymmetric and symmetric C–H vibrations of the methylene groups. The band at 1642 and 1446 cm^{-1} can be ascribed to the asymmetric and symmetric COO^- stretching, respectively.[27,28] Based on the FTIR spectrum, it is interpreted that oleic acid has perhaps capped the surface of the IONPs. In the Ch spectrum, the bands at 1653 and 1594 cm^{-1} (curve ii) are due to the presence of amide I and II groups, respectively.[16] The band at about 1457 cm^{-1} in the spectrum of the PLGA–IONPs (curve iii), assigned to the symmetric CH_2 bending vibration, is found to be shifted to a lower wavenumber (1452 cm^{-1}) in the spectrum of PlgNPs

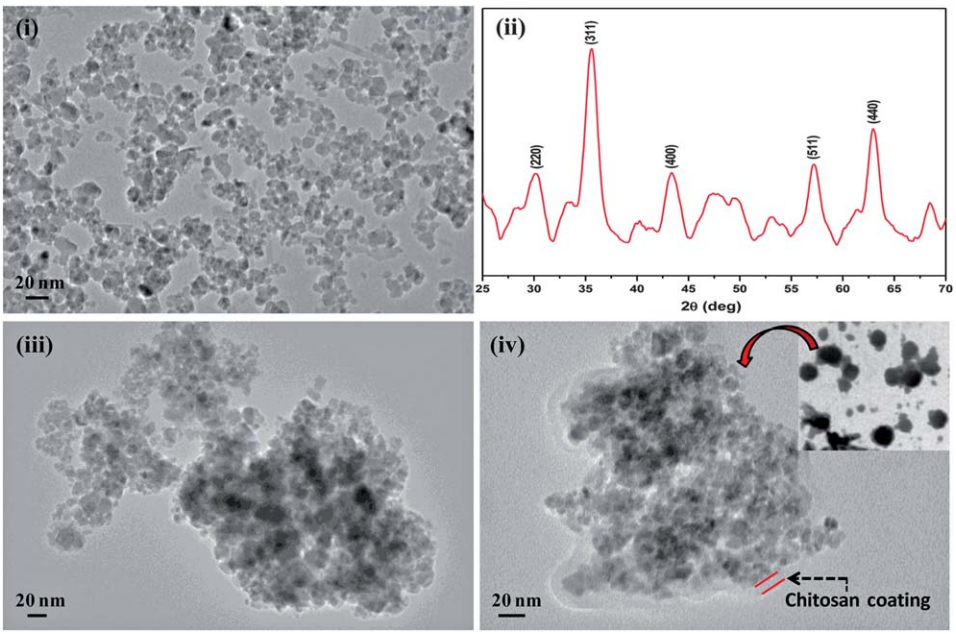

Fig. 1 (i) Transmission electron micrograph (20 nm scale) and (ii) X-ray diffraction pattern of oleic acid-capped IONPs; TEM images of (iii) PLGA–IONPs, and (iv) PlgNPs.

(curve iv) which may be due to the change in conformation of CH_2OH at C-6 position. Further, the peak at 1188 cm^{-1} (curve iv) is attributed to the C–O–C stretch vibration, which arises due to both the bands at 1193 cm^{-1} in the spectrum of the PLGA–IONPs (curve iii) and 1153 cm^{-1} in the spectrum of the Ch (curve ii).

Contact angle studies have been carried out to characterize the immobilization of pDNA onto the PlgNPs/ITO electrode. The CA value of the PlgNPs/ITO electrode is found to be 49.34° (Fig. S1; panel i†), which decreases with increased DNA immobilization. This may be assigned to the enhanced hydrophilicity of the electrode surface after DNA immobilization owing to the presence of the phosphodiester backbone of DNA. The CA measurements were monitored at a regular time interval (1 h), and reveal that the bioelectrode reaches a constant value of 27.39° (Fig. S1; panel ii†) after about 5 h (Fig. S1; panel iii†), indicating that the complete immobilization of the probe has occurred. However, it may be noted that the CA value does not approach 0° after DNA immobilization, which may be due to the presence of the aromatic ring structure of nitrogenous bases present in the nucleic acid.

SEM images of the PlgNPs/ITO electrode (Fig. 4; panel i and ii) indicate the presence of the well-isolated microspheres of PlgNPs, with a mean diameter of about 300 nm. This reveals that during electro-deposition, the PlgNPs do not agglomerate and maintain their spherical shape as the formation of clusters is not observed throughout the electrode surface. However, after incubation of the PlgNPs/ITO electrode with pDNA, the observed variation in morphology may be correlated to the immobilization of pDNA (Fig. 4; panel iii and iv).

Electrochemical impedance spectroscopic analysis after various stages of chemical functionalization, to extract circuit element parameters for the Randles model is depicted in Fig. 5. The interfacial layer at the working electrode is represented by the parallel combination of resistance, which models charge transfer across the functionalized layer, and capacitance C_{dl}, which accounts for the electrical double layer that is formed at the interface. The series impedance Z_w is the standard Warburg term that describes concentration depletion of the redox species near the interface. EIS measures Z_{re} *versus* Z_{im} that can be plotted as a Nyquist diagram which typically exhibits two important regions for a reversible reaction at a solid interface. As indicated in the sketch, the semicircle obtained at high modulation frequency describes the Faradic electron-transfer process at the electrode, whereas the straight region obtained for the lower modulation frequency contains information about the diffusion-limited transport of the redox species in the electrolyte to the electrode interface. We have utilized the semicircle diameter to observe the change of electronic transfer resistance (R_{CT}). After electrophoretic deposition of PlgNPs onto the ITO surface, an R_{CT} value for the PlgNPs/ITO electrode is obtained as 0.7 kΩ (curve i). When the pDNA is immobilized on the electrode surface, the electron-transfer by the negatively charged redox marker, $[Fe(CN)_6]^{3-/4-}$, is hindered resulting in an increased R_{CT} (1.1 kΩ, curve ii) as compared to that of the PlgNPs/ITO electrode.

The results of cyclic voltammetric studies obtained as a function of scan rate (υ, 10–300 mV s^{-1}) for the pDNA/PlgNPs/ITO electrode are shown in Fig. S2.† The positive and negative peaks correspond to the oxidation and reduction reactions of the $[Fe(CN)_6]^{3-/4-}$ redox pair, respectively. The peak currents I_p for both oxidation and reduction follow a linear relation with respect to the square root of scan rate (Fig. S2; inset i†) indicating the existence of diffusion-controlled electrochemical reaction rates for the redox pair at the electrode. It can be seen that the oxidation peak shifts to a more positive value and the

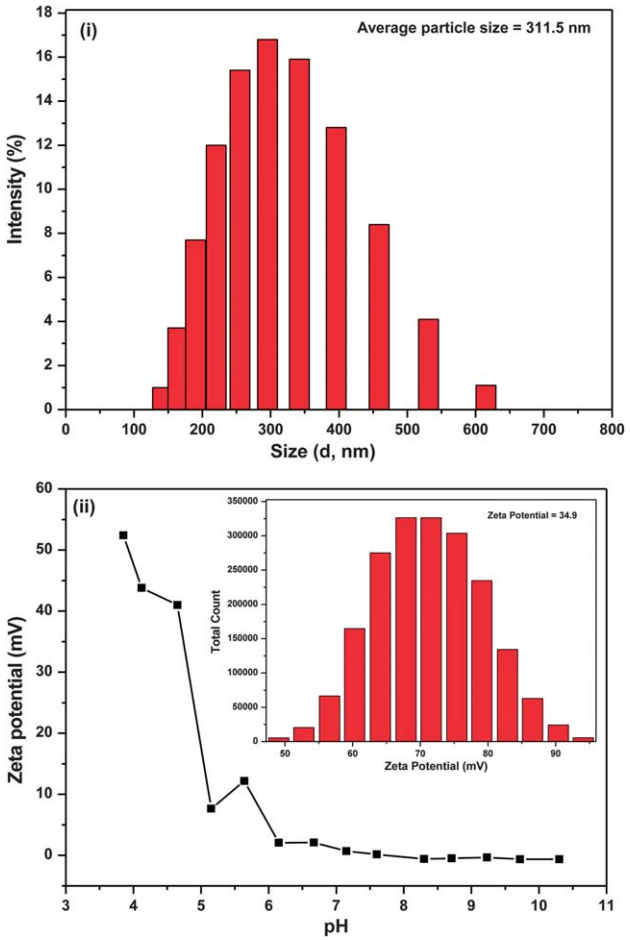

Fig. 2 DLS measurements of PlgNPs showing (i) particle size distributions and (ii) zeta potential values as a function of pH. Inset figure shows the zeta potential measurement of PlgNPs at pH 4.0.

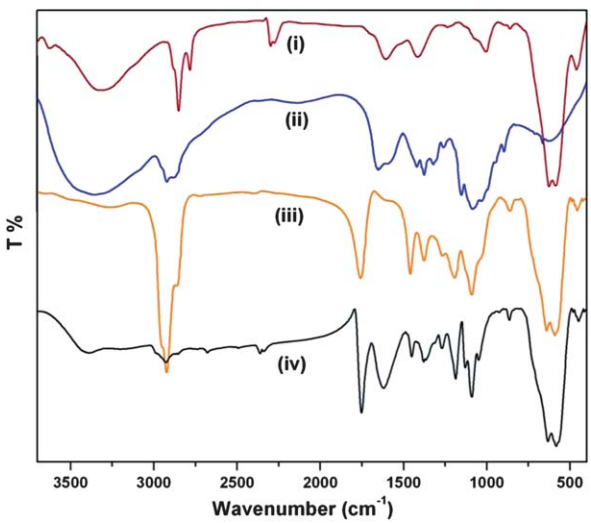

Fig. 3 FTIR spectra of (i) oleic acid-capped IONPs, (ii) chitosan, (iii) PLGA–IONPs, and (iv) PlgNPs.

reduction peak to more negative values with increase of the scan rate and both the peak potentials are linearly dependent on the log of the scan rate (Fig. S2; inset ii†), which agrees well with Laviron's theory[29] and may be given as:

$$E_{pa} = E^{o} + X\ln[(1 - \alpha)Fv/RTk_s] \quad (1)$$

$$E_{pc} = E^{o} + Y\ln[(\alpha)Fv/RTk_s] \quad (2)$$

$$\ln k_s = \alpha\ln(1 - \alpha) + (1 - \alpha)\ln \alpha - \ln(RT/nFv) - \alpha(1 - \alpha)nF\Delta E_p/RT \quad (3)$$

where α and k_s are the electron transfer coefficient and charge transfer rate constant, respectively.[29,30] The plot of ln v *versus* the anodic peak potential (E_{pa}) and cathodic peak potential (E_{pc}) yields two straight lines with their slopes of $X = RT/(1 - \alpha)nF$ and $Y = RT/\alpha nF$, respectively. Based on the plot (Fig. S2; inset ii†) and eqns (1) and (3), the values of α and k_s have been determined as 0.64 and 61.73 s^{-1}, respectively. According to Laviron's equation, the relationship between peak current (I_p) and surface coverage can be described as:

$$I_p = n^2F^2vA\Gamma(4RT)^{-1} \quad (4)$$

where, I_p is peak current, n is the number of electrons transferred, v is the scan rate (50 mV s^{-1}), A is the electrode area (0.25 cm^2), and Γ is the average surface coverage of the electrode redox substance (mol cm^{-2}). Taking the average of both the cathodic and anodic results, Γ is found to be 1.07×10^{-7} mol cm^{-2}. On the basis of the linear slope of the anodic peak currents on the square root of the potential sweep rates, and the Randles–Sevcik equation,[31]

$$I_p = (2.99 \times 10^5)\alpha^{1/2}n^{3/2}ACD^{1/2}v^{1/2} \quad (5)$$

the diffusion coefficient (D) is calculated as 2.26×10^{-10} cm^2 s^{-1}. Here n is the number of transferred electrons for the redox reaction, C is the molar concentration of $[Fe(CN)_6]^{3-/4-}$, and v is the scan rate (50 mV s^{-1}). By performing a linear regression for I_p *versus* $v^{1/2}$, the slope S can be obtained and the effective surface area of the electrode (A) is calculated to be 0.73 mm^2 using eqn (6):[32,33]

$$A = S/(2.99 \times 10^5)n^{3/2}\alpha^{1/2}CD^{1/2} \quad (6)$$

For comparison, control experiments have been carried out using the pDNA/Ch–IONPs/ITO bioelectrode and the values obtained are given in Table 1. The improved kinetics of pDNA/PlgNPs/ITO compared to that of the pDNA/Ch–IONPs/ITO bioelectrode may perhaps be due to better dispersion of IONPs in PlgNPs than in pristine chitosan. This uniform distribution may be attributed to the fact that carboxylate and hydroxyl terminal groups of PLGA have strong coordination with the surface of the IONPs.[9–11] However, in the Ch–IONPs composite, the IONPs are dispersed merely due to electrostatic interactions, resulting in the entrapment of IONPs within the polymer matrix.

The DNA hybridization on the modified electrode has been verified by EIS, which is known to be very sensitive to changes in

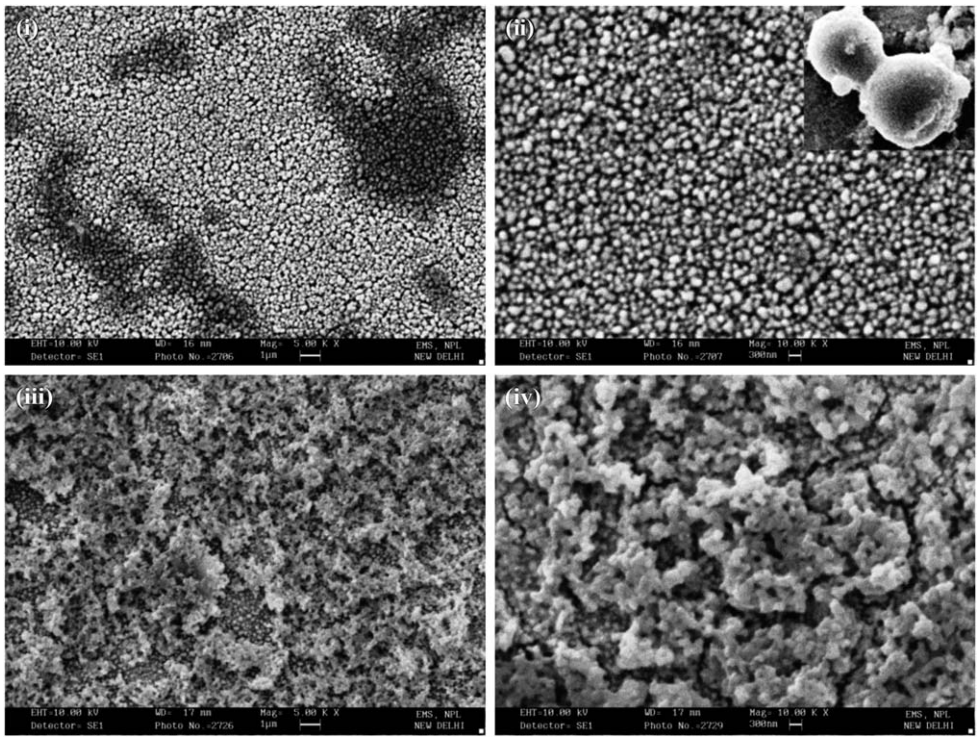

Fig. 4 SEM images of (i and ii) PlgNPs/ITO electrode and (iii and iv) pDNA/PlgNPs/ITO bioelectrode at magnifications of 5 k× and 10 k× respectively.

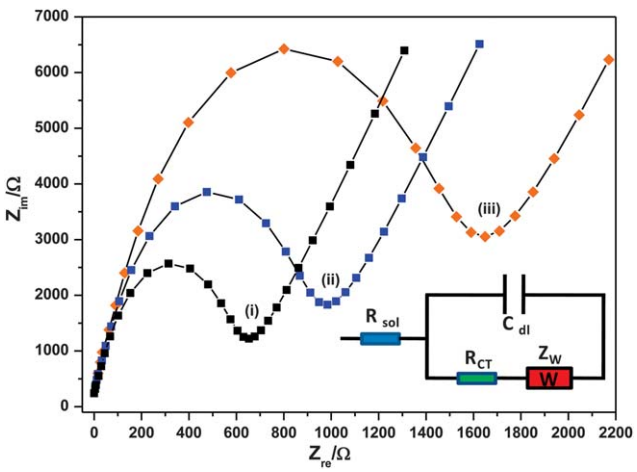

Fig. 5 Nyquist diagram (Z_{im} *versus* Z_{re}) for the Faradic impedance measured in PBS solution (pH 7.4) containing 5 mM $[Fe(CN)_6]^{3-/4-}$, in the frequency range from 10^6 to 10^{-2} Hz for (i) PlgNPs/ITO electrode, (ii) pDNA/PlgNPs/ITO bioelectrode, and (iii) cDNA on pDNA/PlgNPs/ITO bioelectrode.

interfacial impedance upon bio-recognition events occurring at the surface/electrolyte interface.[34] As mentioned earlier, when pDNA is immobilized onto the PlgNPs/ITO electrode, an increase in R_{CT} value is observed which may be due to the negatively charged phosphate backbone of pDNA exposed to the electrolyte, which in turn perhaps repel $[Fe(CN)_6]^{3-/4-}$. When the pDNA is incubated with its complementary target DNA sequence (cDNA), the hybridization reaction occurs and more negatively charged phosphate backbones are introduced, hence the R_{CT} value increases following the formation of double-stranded DNA (Fig. 5, curve iii). It can thus be inferred that with a change in negative-charge and conformation transition, there is a change in the interfacial properties. With increase of the cDNA concentration, the R_{CT} value increases correspondingly (Fig. 6, curve ix–i). The difference between the value of R_{CT} for the pDNA immobilized electrode and after hybridization with cDNA ($\Delta R_{CT} = R_{CT}$cDNA $- R_{CT}$pDNA) has been used as the measurement signal. The analytical signal (in terms of ΔR_{CT}) shows linear relationship with the logarithmic value of the complementary target DNA concentration ranging from 10^{-13} to 10^{-6} M (Fig. S3†) and follows the following equation:

$$\Delta R_{CT} = 73.030 \log C + 1028.957 \quad (7)$$

with a linear regression coefficient of 0.994. The detection limit is calculated to be 8.7×10^{-14} M using the expression 3σ/sensitivity, where σ is standard deviation.

Table 1 Kinetic parameters calculated for the fabricated bioelectrodes

Sl. no	Name of the electrode	Electron transfer coefficient, α	Charge transfer rate constant, k_s/s^{-1}	Effective surface area, A_{eff}/mm^2	Average surface coverage, Γ/mol cm^{-2}	Diffusion coefficient, $D/cm^2\ s^{-1}$
1	pDNA/PlgNPs/ITO	0.64	61.73	0.73	1.07×10^{-7}	2.26×10^{-10}
2	pDNA/Ch–IONPs/ITO	0.57	28.90	0.33	6.46×10^{-8}	1.45×10^{-10}

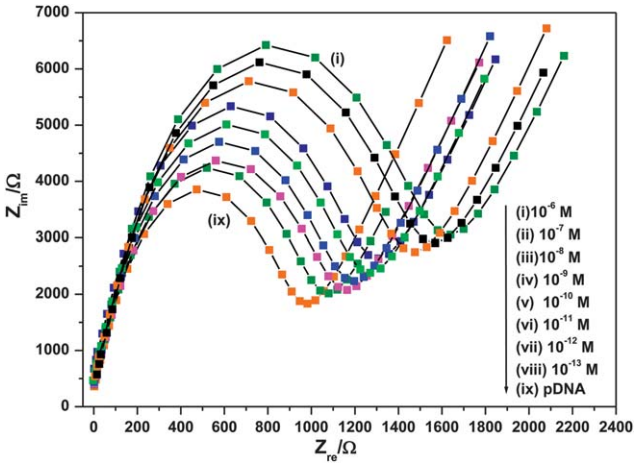

Fig. 6 EIS response of pDNA/PlgNPs/ITO bioelectrode as a function of cDNA concentration (10^{-13} to 10^{-6} M) in PBS solution (pH 7.4) containing 5 mM $[Fe(CN)_6]^{3-/4-}$.

Selectivity of the pDNA/PlgNPs/ITO bioelectrode towards non-complementary, one-base mismatch sequences and various water-borne pathogens (*Salmonella typhimurium*, *Neisseria meningitides*, *Shigella dysenteriae*, *Clostridium botulinum* and *Klebsiella pneumonia*) has been further studied using EIS (Fig. 7). When the pDNA/PlgNPs/ITO bioelectrode is treated with the non-complementary DNA, a negligible increase in R_{CT} value is observed (ΔR_{CT} = 28.49 Ω). Since, the non-complementary DNA bases do not match with the pDNA bases, it is expected that there is no duplex formation and hence the R_{CT} value remains unvaried. When the pDNA/PlgNPs/ITO bioelectrode is incubated with the single-base mismatch DNA sequence, a significant value of ΔR_{CT} (149.28 Ω) is obtained. This may be due to the partial hybridization of pDNA that results in a slight increase of negative charge on the bioelectrode surface, leading to repulsion of $[Fe(CN)_6]^{3-/4-}$ redox ions. Specificity studies have been conducted by isolating DNA from a panel of strains of *E. coli*, and other water-borne pathogens as shown in the bar diagram. A marked increase of 549.98 Ω in the R_{CT} value is seen after incubation of the bioelectrode with the clinical *E. coli* strain, which indicates complete hybridization. A negligible change in R_{CT} value is noticed for pDNA/PlgNPs/ITO bioelectrode after incubation with clinical samples of other water-borne pathogens, revealing the specificity of this biosensor for *E. coli* detection.

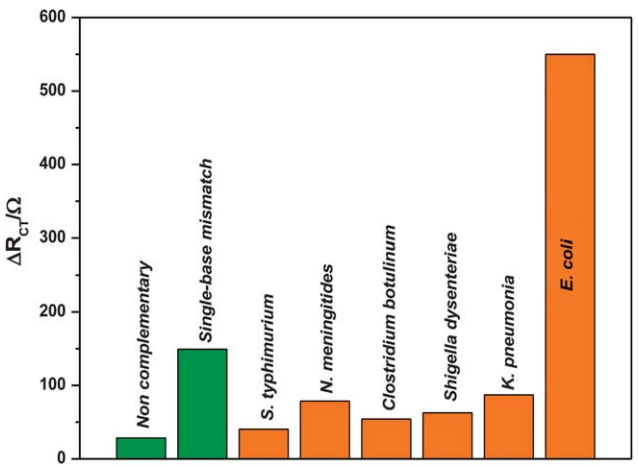

Fig. 7 Bar diagram showing the impedimetric response (in terms of ΔR_{CT}) of pDNA/PlgNPs/ITO bioelectrode incubated with (i) non-complementary, (ii) single-base mismatch, and (iii–viii) DNA extracted from culture of water-borne pathogens.

Regeneration studies have been performed by immersing the fabricated bioelectrode into Tris–EDTA buffer solution (pH 8.0) at 100 °C for 5 min, followed by cooling in the ice bath for about 30 min.[20] The results obtained for each successive denaturation and regeneration process have been plotted in terms of ΔR_{CT} *versus* the number of detection cycles. It is found that the ΔR_{CT} value for the bioelectrode decreases after each cycle and reduces to about 81% of the initial value (1st cycle) after eight regeneration processes (Fig. S4†). Also, it is to be mentioned that the R_{CT} value of the bioelectrode slightly increased with each consecutive measurement, whereas a decrease in the R_{CT} value is obtained after hybridization. The slight increase in R_{CT} value after each denaturation process may be assigned to the incomplete denaturation at the bioelectrode surface,[35] which might lead to a reduced hybridization efficiency thereby resulting in a decreased R_{CT} value after hybridization. Further, the stability of the fabricated DNA biosensor has been investigated *via* EIS after its hybridization with complementary target DNA. It is found that the bioelectrode retains about 95% of its initial response after about 6 weeks, when stored at 4 °C (data not shown). These results indicate that the label-free EIS strategy based on the PlgNPs/ITO electrode has scope to detect cDNA in a wide concentration range and has a good reusability in comparison to other reported nanomaterials-based impedimetric DNA sensors (Table S2†).[36–38]

Conclusions

Cationic poly(lactic-*co*-glycolic acid) iron oxide hybrid microspheres have been synthesized by the nano-emulsion method. TEM examination of the particles gives strong evidence for the presence of nanoscale iron oxide within the polymer matrix. These nano-composites are nearly spherical in shape with a mean size of 310 nm. The prepared microspheres provide an excellent platform for DNA immobilization when they are electrophoretically deposited onto an ITO-coated glass electrode. The fabricated biosensor is found to exhibit good selectivity for *E. coli* detection and retains significant activity (81% of the initial activity) after 9 cycles of use. The experiments relating to studies of device performance with respect to change in the size of the microspheres, compositions of PLGA and IONPs and electro-deposition parameters are in progress. Further, results of these studies have implications towards the application of these biocompatible microspheres in magnetic-field-assisted drug delivery systems, cell/enzyme immobilization, and many other biomedical related fields.

Acknowledgements

We thank Director, NPL, New Delhi, India for the facilities. C.M.P. and A.S. are thankful to CSIR, India, for the award of SRF. Thanks are due to Dr. Seema Sood for providing the bacterial culture samples and Dr. Ashutosh Kumar Pandey (AIIMS, New Delhi, India) for the useful discussions. The financial support received from Department of Science and Technology, India (Grant No. DST/TSG/ME/2008/18) and Indian Council of Medical Research, India (Grant No. ICMR/5/3/8/91/GM/2010-RHN) is gratefully acknowledged.

References

1 S. F. Medeiros, A. M. Santos, H. Fessi and A. Elaissari, *Int. J. Pharm.*, 2011, **403**, 139–161.
2 M. Corti, A. Lascialfari, E. Micotti, A. Castellano, M. Donativi, A. Quarta, P. D. Cozzoli, L. Manna, T. Pellegrino and C. Sangregorio, *J. Magn. Magn. Mater.*, 2008, **320**, e320–e323.
3 Y. W. Jun, Y. M. Huh, J. S. Choi, J. H. Lee, H. T. Song, S. Yoon, K. S. Kim, J. S. Shin, J. S. Suh and J. Cheon, *J. Am. Chem. Soc.*, 2005, **127**, 5732–5733.
4 P. R. Solanki, A. Kaushik, V. V. Agrawal and B. D. Malhotra, *NPG Asia Mater.*, 2011, **3**, 17–24.
5 J. Wang, A. N. Kawde, A. Erdem and M. Salazar, *Analyst*, 2001, **126**, 2020–2024.
6 M. Pauly, B. P. Pichon, P. Panissod, S. Fleutot, P. Rodriguez, M. Drillon and S. Begin-Colin, *J. Mater. Chem.*, 2012, **22**, 6343–6350.
7 J. E. Wong, A. K. Gaharwar, D. Müller-Schulte, D. Bahadur and W. Richtering, *J. Colloid Interface Sci.*, 2008, **324**, 47–54.
8 A. K. Gupta and M. Gupta, *Biomaterials*, 2005, **26**, 3995–4021.
9 M. Kim, Y. Chen, Y. Liu and X. Peng, *Adv. Mater.*, 2005, **17**, 1429–1432.
10 G.-D. Fu, G. L. Li, K. G. Neoh and E. T. Kang, *Prog. Polym. Sci.*, 2011, **36**, 127–167.
11 M. N. V. Ravi Kumar, U. Bakowsky and C. M. Lehr, *Biomaterials*, 2004, **25**, 1771–1777.
12 C. Foged, B. Brodin, S. Frokjaer and A. Sundblad, *Int. J. Pharm.*, 2005, **298**, 315–322.
13 K. Tahara, T. Sakai, H. Yamamoto, H. Takeuchi, N. Hirashima and Y. Kawashima, *Int. J. Pharm.*, 2009, **382**, 198–204.
14 Y. Wang, A. S. Angelatos and F. Caruso, *Chem. Mater.*, 2007, **20**, 848–858.
15 J. R. Grech, J. Mano and R. Reis, *J. Mater. Sci.: Mater. Med.*, 2010, **21**, 1855–1865.
16 Z. Liu, H. Wang, B. Li, C. Liu, Y. Jiang, G. Yu and X. Mu, *J. Mater. Chem.*, 2012, **22**, 15085–15091.
17 A. Sharma, C. M. Pandey, Z. Matharu, U. Soni, S. Sapra, G. Sumana, M. K. Pandey, T. Chatterjee and B. D. Malhotra, *Anal. Chem.*, 2012, **84**, 3082–3089.
18 A. R. Boccaccini, S. Keim, R. Ma, Y. Li and I. Zhitomirsky, *J. R. Soc., Interface*, 2010, **7**, S581–S613.
19 A. Sharma, C. M. Pandey, G. Sumana, U. Soni, S. Sapra, A. K. Srivastava, T. Chatterjee and B. D. Malhotra, *Biosens. Bioelectron.*, 2012, **38**, 107–113.
20 C. M. Pandey, R. Singh, G. Sumana, M. K. Pandey and B. D. Malhotra, *Sens. Actuators, B*, 2011, **151**, 333–340.
21 S. Sun, H. Zeng, D. B. Robinson, S. Raoux, P. M. Rice, S. X. Wang and G. Li, *J. Am. Chem. Soc.*, 2003, **126**, 273–279.
22 R. A. Wassel, B. Grady, R. D. Kopke and K. J. Dormer, *Colloids Surf., A*, 2007, **292**, 125–130.
23 H. Zhao, K. Saatchi and U. O. Häfeli, *J. Magn. Magn. Mater.*, 2009, **321**, 1356–1363.
24 C. M. Pandey, G. Sumana and B. D. Malhotra, *Biomacromolecules*, 2011, **12**, 2925–2932.
25 S. J. Lee, J. R. Jeong, S. C. Shin, J. C. Kim, Y. H. Chang, K. H. Lee and J. D. Kim, *Colloids Surf., A*, 2005, **255**, 19–25.
26 A. Corrias, G. Mountjoy, D. Loche, V. Puntes, A. Falqui, M. Zanella, W. J. Parak and M. F. Casula, *J. Phys. Chem. C*, 2009, **113**, 18667–18675.
27 L. M. Bronstein, X. Huang, J. Retrum, A. Schmucker, M. Pink, B. D. Stein and B. Dragnea, *Chem. Mater.*, 2007, **19**, 3624–3632.
28 A. Hofmann, S. Thierbach, A. Semisch, A. Hartwig, M. Taupitz, E. Ruhl and C. Graf, *J. Mater. Chem.*, 2010, **20**, 7842–7853.
29 E. Laviron, *J. Electroanal. Chem.*, 1979, **100**, 263–270.
30 G. Karim-Nezhad, M. Hasanzadeh, L. Saghatforoush, N. Shadjou, S. Earshad and B. Khalilzadeh, *J. Braz. Chem. Soc.*, 2009, **20**, 141–151.
31 A. J. Bard and L. R. Faulkner, *Electrochemical Methods*, John Wiley and Sons, New York, 2001.
32 J. Shi, J. C. Claussen, E. S. McLamore, A. ul Haque, D. Jaroch, A. R. Diggs, P. Calvo-Marzal, J. L. Rickus and D. M. Porterfield, *Nanotechnology*, 2011, **22**, 355502–355502.
33 I. Tiwari and M. Singh, *Microchim. Acta*, 2011, **174**, 223–230.
34 Y. Hu, F. Li, X. Bai, D. Li, S. Hua, K. Wang and L. Niu, *Chem. Commun.*, 2011, **47**, 1743–1745.
35 Y. Xu, H. Cai, P. G. He and Y. Z. Fang, *Electroanalysis*, 2004, **16**, 150–155.
36 N. Zhou, T. Yang, Y. Zhang, C. Jiang and K. Jiao, *Thin Solid Films*, 2009, **518**, 338–342.
37 Y. Chen, B. Jiang, Y. Xiang, Y. Chai and R. Yuan, *Chem. Commun.*, 2011, **47**, 12798–12800.
38 N. Zhou, T. Yang, C. Jiang, M. Du and K. Jiao, *Talanta*, 2009, **77**, 1021–1026.